AGU PUBLICATIONS

Geophysical Research Letters

RESEARCH LETTER

10.1002/2014GL062020

Key Points:
- Periodic dispersive features are observed in the fast magnetosonic mode
- Dispersive feature suggests fairly localized wave source
- The cause of the modulation of the wave source remains to be identified

Correspondence to:
S. A. Boardsen,
Scott.A.Boardsen@nasa.gov

Citation:
Boardsen, S. A., G. B. Hospodarsky, C. A. Kletzing, R. F. Pfaff, W. S. Kurth, J. R. Wygant, and E. A. MacDonald (2014), Van Allen Probe observations of periodic rising frequencies of the fast magnetosonic mode, *Geophys. Res. Lett.*, *41*, 8161–8168, doi:10.1002/2014GL062020.

Received 29 SEP 2014
Accepted 5 NOV 2014
Accepted article online 7 NOV 2014
Published online 2 DEC 2014

Van Allen Probe observations of periodic rising frequencies of the fast magnetosonic mode

S. A. Boardsen[1,2], G. B. Hospodarsky[3], C. A. Kletzing[3], R. F. Pfaff[2], W. S. Kurth[3], J. R. Wygant[4], and E. A. MacDonald[2]

[1]Goddard Planetary Heliophysics Institute, University of Maryland, Baltimore County, Maryland, United States, [2]NASA/GSFC, Greenbelt, Maryland, United States, [3]Department of Physics and Astronomy, University of Iowa, Iowa City, Iowa, United States, [4]Department of Physics and Astronomy, University of Minnesota Twin Cities, Minneapolis, Minnesota, United States

Abstract Near simultaneous periodic dispersive features of fast magnetosonic mode emissions are observed by both Van Allen Probes spacecraft while separated in magnetic local time by ~5 h: Probe A at 15 and Probe B at 9–11 h. Both spacecraft see similar frequency features, characterized by a periodic repetition at ~180 s. Each repetition is characterized by a rising frequency. Since no modulation is observed in the proton shell distribution, the plasma density, or in the background magnetic field at either spacecraft we conclude that these waves are not generated near the spacecraft but external to both spacecraft locations. Probe A while outside the plasmapause sees the start of each repetition ~40 s before probe B while deep inside the plasmasphere. We can qualitatively reproduce the dispersive features but not the quantitative details. The cause for this phenomena remains to be identified.

1. Introduction

Fast magnetosonic waves are often observed around the Earth's inner equatorial magnetosphere and occur mainly at frequencies (f) between the proton cyclotron frequency (f_{cP}) and the lower hybrid frequency (f_{LHR}) [e.g., *Santolík et al.,* 2004; *Meredith et al.,* 2008]. The occurrence of these waves is usually concentrated around the plasmapause, and they are observed more often on the dayside [e.g., *Meredith et al.,* 2008]. At geosynchronous orbit the local time distribution (not normalized by coverage) of this mode is given in Figure 9 of *Korth et al.* [1984], the primary peak is at around noon, with a narrow secondary peak at midnight. In that study time series, magnetometer data with a Nyquist frequency of 12 Hz were used to identify this mode so $f_{cP}/f < 10$. The wave magnetic field is strongly aligned with the background magnetic field (large magnetic compressibility $(\delta b_{||}/\delta b)^2 > 0.8$) and therefore the wave normal angle (WNA) is near 90°. The wave electric field is nearly perpendicular to the background magnetic field and is nearly aligned with the wave vector. At ~0.5 f_{cP} the longitudinal electric field is approximately equal to the transverse electric field, and as f approaches f_{LHR} the electrostatic component of the waves becomes dominant (Figure 1a).

The source of the instability is believed to be proton shell distributions [e.g., *Perraut et al.,* 1982; *Boardsen et al.,* 1992; *Chen et al.,* 2011; *Thomsen et al.,* 2011]. When the perpendicular component of the phase velocity lies in the region of positive perpendicular slope of the proton shell distribution, this distribution can become unstable to these waves. The peak wave growth is near WNA ~ 89.95°, very close to the point where these waves refract back toward the magnetic equator (WNA = 90°) and peak damping occurs while crossing the magnetic equator where the wave normal angle has the strongest deviation up to ~2° away from 90° [*Boardsen et al.,* 1992]. Electron temperature strongly influences the peak wave growth and is a strong contributor to the Landau damping [*Horne et al.,* 2000]. For a fixed proton shell distribution the band of harmonic emissions around peak growth rate shifts in frequency as V_A shifts, as shown in Figure 9 of *Boardsen et al.* [1992].

The radial and azimuthal propagations of these waves are influenced by the large-density gradients present at the plasmapause, which produces a local maximum in the index of refraction that can act as a wave guide oriented roughly in the azimuthal direction [e.g., *Chen and Thorne*, 2012]. The radial extent of the wave guide can be large: *Ma et al.* [2014] shows examples where the radial extent of the wave guide is ~1.5 R_E. The latitudinal propagation of these waves is determined by the equatorial WNA. *Boardsen et al.* [1992] showed that for WNA not equal to 90° (i.e., 89°) as the wave frequency approaches f_{LHR} (~42 f_{cP}) the group velocity becomes strongly field aligned, and these waves will propagate back and forth across the magnetic equator

©2014. American Geophysical Union. All Rights Reserved.

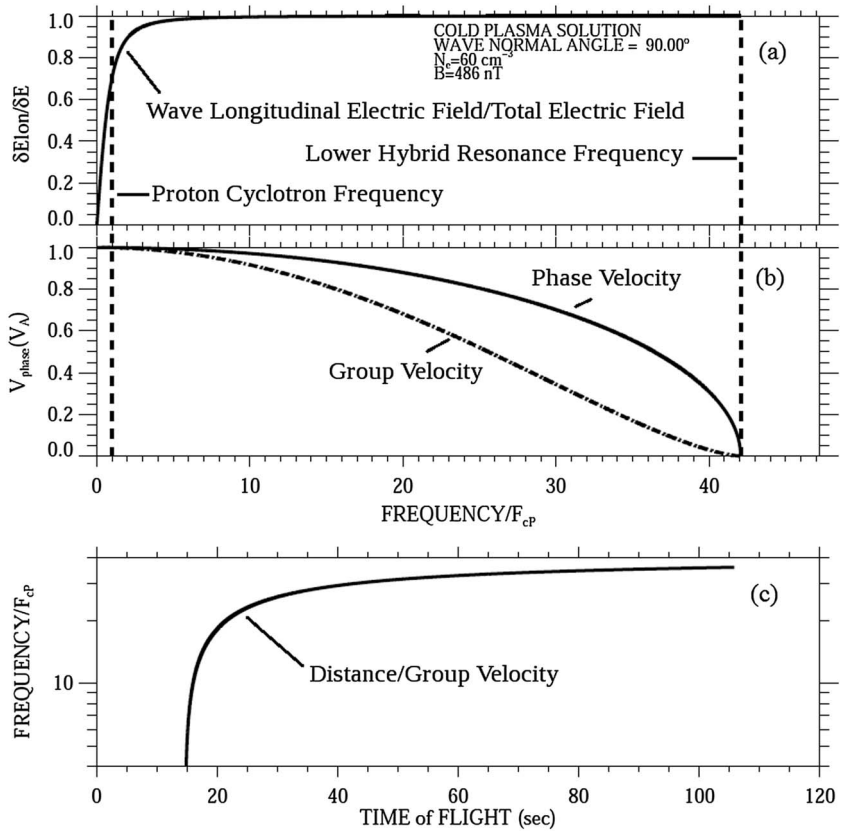

Figure 1. Cold plasma solution of the fast magnetosonic mode for a 100% proton ion composition, N_e = 60 cm^{-3}, and B = 486 nT. (a) Ratio of the wave longitudinal to total electric field. (b) Phase (solid) and group velocity (dashed) versus f/f_{cP}. (c) The propagation time versus f/f_{cP} for waves launched at noon, at the magnetic equator, and in the azimuthal direction, to Probe A at 15 MLT, for an azimuthally symmetrical density and magnetic field model.

and drift either in the radial direction or in magnetic local time (MLT), depending on the azimuthal orientation of the wave vector. By modeling the observed radiation pattern using plasma wave ray tracing, *Boardsen et al.* [1992] estimated that at the magnetic equator the WNA > 88° and for large f/f_{cP} (>10) the waves are observed to propagate up to magnetic latitudes of ±10°.

We present an event study of periodic dispersive rising frequency emissions of the fast magnetosonic mode detected by both Van Allen Probe spacecraft, while separated by ~5 h MLT. Observations of modulated chorus [e.g., *Li et al.,* 2011], modulated plasmaspheric hiss [e.g., *Chen et al.*, 2012], and modulated ion cyclotron waves [e.g., *Loto'aniu et al.,* 2009] have been discussed in previous works, but to our knowledge, periodic dispersive frequency features in the fast magnetosonic have not been reported in the literature.

2. Observations

The data used in this study are from the Electric and Magnetic Field Instrument and Integrated Science suite [*Kletzing et al.,* 2013], which is composed of a flux gate magnetometer and the Waves instrument comprising a six-channel Waveform Frequency Receiver (WFR), and a High Frequency Receiver (HFR). The flux gate magnetometer measures the background magnetic field at 64 samples per second. In the survey mode the WFR measures all six E and B field components at 65 quasi-log-spaced frequencies ranging from 2 Hz to 11 kHz at a 6 s cadence and is used to detect the fast magnetosonic mode emissions. The HFR measures one E field component at 80 frequencies ranging from 10 kHz to 500 kHz and is used to determine the electron density by measuring the upper hybrid resonance frequency (f_{UHR}). We also use the Electric Field and Waves Instrument [*Wygant et al.,* 2013], which measures spacecraft minus probe potential (which can be used to estimate the plasma density) and the Helium Oxygen Proton Electron particle instrument [*Funsten et al.,* 2013], which measures H^+, He^+, O^+, and electrons in the energy range of a few eV to ~40 keV.

©2014. American Geophysical Union. All Rights Reserved.

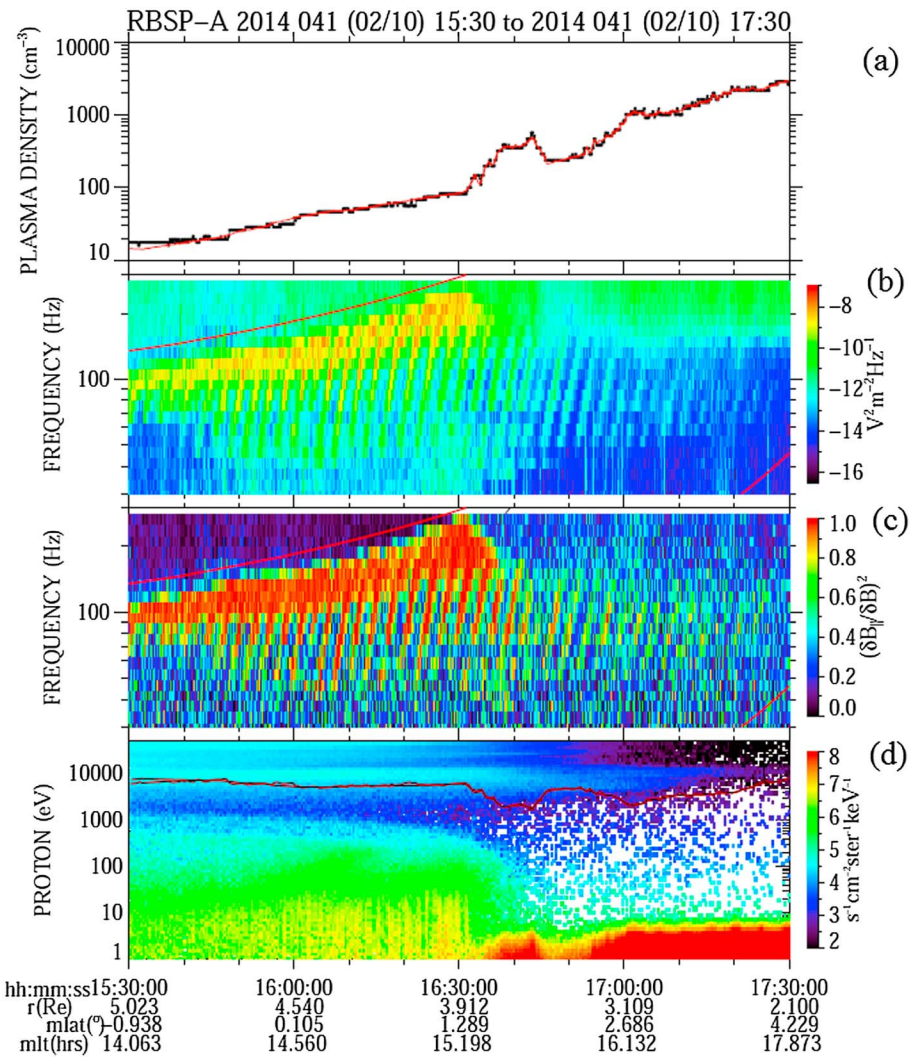

Figure 2. (a) Plasma density inferred from the f_{UHR} (black) and spacecraft potential (red), (b) electric field power spectral density from the spin plane antennas, (c) magnetic compressibility, and (d) the omnidirectional proton differential flux; the upper line is at 1/2 $m_p V_A^2$. The top line in Figures 2a and 2b is at the f_{LHR} (~42 f_{cP}) and the bottom line is at f_{cP}. The inbound plasmapause crossing is near 16:30 UT.

Having noticed a few examples of modulated fast magnetosonic waves in the data, we visually searched the data set for examples of these events finding about 100 such events. We are preparing general survey paper on fast magnetosonic waves by the Van Allen Probes that will include a comparison of events with no discernible modulation with those with modulation. We chose the event in this study because the periodic features are clearly delineated in the probe A observations, and probe A and B are widely separated in magnetic local time.

Van Allen Probe observations of these waves are shown in Figures 2 and 3. The plasmapause crossing, loosely defined as the position where the plasmas density rises above 100 cm^{-3}, for Probe A is at ~16:30 UT at r = 3.9 R_E and MLT = 15.2 h, while that of probe B is at ~17:30 UT at r = 4.7 R_E and MLT = 10.7 h. Below f_{LHR} both probes see repetitive rising frequency emissions with a repetition period of ~180 s. The magnetic compressibility of these repeated rising frequency emissions is near 1, consistent with the wave characteristics of the fast magnetosonic mode (Figures 2 and 3c). The compressibility becomes less pronounced and disappears inside the plasmasphere as the magnetic wave intensity drops below the instrumental noise level.

For Probe A (Figure 2b) the repetitive rising frequency emissions cross the plasmapause with no discernible change in the timing of the repetition. While for Probe B (Figure 3b) this pattern is observed deep inside the plasmasphere form 16:00 to 16:40 UT, followed by a gap between 16:40 and 17:30 UT where no emissions are

©2014. American Geophysical Union. All Rights Reserved.

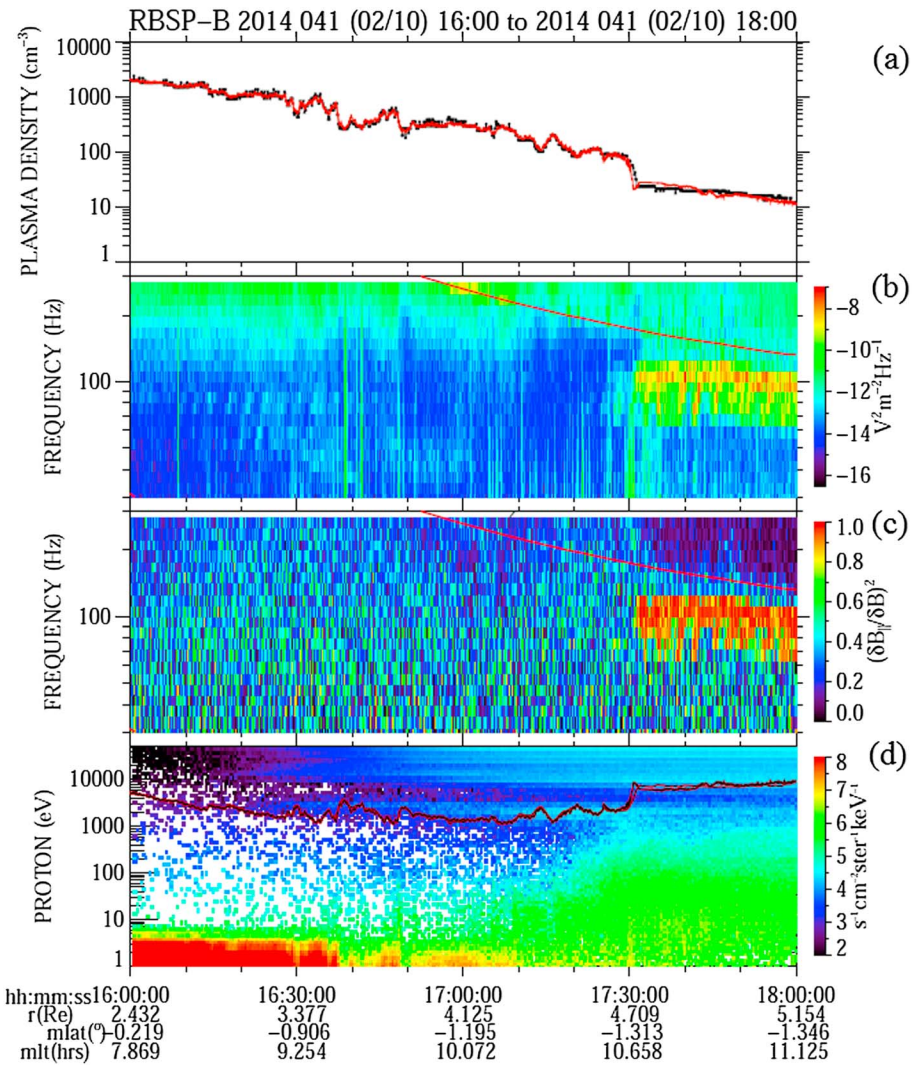

Figure 3. (a–d) Probe B measurements are shown whose time range overlaps with that of Probe A as shown in Figure 2. The outbound plasmapause crossing by Probe B is near 17:30 UT.

observed, and the waves pick up again outside the plasmapause. Probe B sees only one repeated pattern just inside the plasmapause. The inner magnetospheric wave guide does not exclude magnetosonic waves generated near or outside the plasmapause from penetrating deep inside the plasmasphere. For example, the trapped region in *Chen and Thorne* [2012] is between 2.5 and 4.5 R_E (see Figure 2 of that paper), and density variations can be present that can refract these waves in azimuth toward wave normal angles nearer 0° or 180° where those rays can escape the duct.

The reason why Probe A sees no gap in emissions and Probe B sees a big gap must be due to differences in propagation between the source and the observations. The gradual density increase across the plasmapause for Probe A will lead to gradual changes in the wave propagation. The sharp density increase across the plasmapause at Probe B will have a tendency to focus the rays in the radial direction as they propagate inward. We believe the lack of waves just inside the plasmapause at Probe B is due to the strong azimuthal orientation of the wave vector. For Probe B the median orientation of the wave electric field (proxy for the wave vector direction, see Figure 1a) is 29° from the azimuthal direction, while at Probe A it is 20°. Ray tracing is required to fully understand the presence of the gap.

Above 2 keV, proton shell distributions are observed by both spacecraft (Figures 2d and 3d); however, these distributions weaken inside the plasmasphere. Outside the plasmapause the 1/2 $m_p V_A^2$ line lies within the

©2014. American Geophysical Union. All Rights Reserved.

shell distribution, suggesting that a local instability can exist, while inside the plasmapause, the 1/2 $m_p V_A^2$ line tends to lie below the proton shell distribution suggesting that the waves are generated elsewhere. If V_A lies below the region of positive slope in the shell distribution the instability cannot occur. If V_A, because the phase velocity drops to zero as the lower hybrid frequency is approached (Figure 1b), lies somewhere in the shell distribution or above, it is possible that the instability can be local.

However, satisfying the local instability conditions is a necessary but not sufficient condition in order for these waves to tap the free energy of the protons, the waves must also experience sufficient path integrated gain. Waves launched close to the magnetic equator in the azimuthal direction with a wave normal angle (i.e., 89.95°) that satisfies the resonances condition in a region that is locally azimuthally symmetric in density will probably experience the strongest gain. Once the symmetry is broken, the resonance condition will no longer be satisfied because the phase velocity is dependent upon the changing local density and mass distribution. Both probes might be in a region that is not locally azimuthally symmetric in density, therefore the free energy of the protons is not strongly tapped at those locations.

We have found no discernible modulation at ~180 s of the proton shell distribution, of the electron density, of the background magnetic field, or of the background dc electric field suggesting that the waves observed by both Probes A and B are outside the source that is creating the repetitive pattern. Outside the plasmapause both A and B see wave intensities of a similar magnitude, suggesting that the source might be earlier in the afternoon, while the lack of a gap in the emission as detected by Probe A while crossing the plasmapause suggests that the source is closer to Probe A than Probe B.

3. Discussion

We start with the following simple explanation for the dispersive appearance of the frequency emissions. At a WNA of 90°, near f_{cP} the phase and group velocity is near the Alfven velocity (V_A), when f increases toward f_{LHR}, both the phase and group velocity decrease approaching 0 at f_{LHR} (Figure 1b). So as waves propagate away from a "localized equatorial source," they will develop a dispersive signature with the higher-frequency waves arriving at later times than that of a lower frequency waves (Figure 1c). If the "localized source" is being turned on and off by a mechanism that remains to be identified, then a spacecraft outside the source region could detect periodic rising dispersive frequency emissions of the fast magnetosonic mode.

Figure 4 compares observations by Probes A and B over the same 40 min interval. Outside the plasmasphere the emissions observed by Probe A (Figure 4a) are confined in frequency between approximately the eighth and the 36th harmonics of f_{cP}, while inside the plasmasphere the emissions observed by Probe B (Figure 4b) are confined in frequency between approximately the third and ninth harmonics of f_{cP}. Each rising frequency emission observed by Probe A outside the plasmasphere leads those of Probe B inside the plasmasphere by ~40 s (Figure 4c). Outside the plasmapause, V_A is ~1000 km/s at Probe A, assuming 100% H+, for a wave traveling in the azimuthal direction starting at Probe A, the propagation time at 4 R_E from 15 to 9 MLT and the time delay is ~40 s, which suggests that the source might be closer to Probe A than Probe B, but Probe A sees what we interpret to be a strongly dispersive signature suggesting that the source must be away from Probe A. The Alfven velocity inside the plasmasphere is about 500 km/s, so for a source located near noon, the time delay will be similar, since the ray path to Probe B will lie mainly inside the plasmasphere.

The dispersion curve (Figure 1c) is quantitatively similar to the observed rising frequencies (Figure 4a), the flattening of the slope as the wave frequency approaches f_{LHR} is highly suggestive that this is a propagation effect and from a localized source. However, we do not find quantitative consistency between the simple model (distance divided by group velocity) used to create the dispersion curve (Figure 1c) and the observed rising frequency of a repetition (Figure 4a). For example, comparing the rising frequency versus time between Figures 4a and 1c, Probe A sees the frequency rising from ~8 to ~24 f/f_{cP} in 150 s, while the rise time from 8 to 24 f/f_{cP} in Figure 1 is 13 s, a factor of 10 difference! One way to get a closer agreement is to increase the plasma density by a factor of 100, but this is not consistent with observations. Including O+ at say 90% would reduce the factor to 2.5, but such high levels of O+ are unrealistic. Doubling the difference in MLT between source and observer would reduce the difference of the factor to 5.0, but a source location at 21 MLT seems unrealistic, and a source at 9 MLT seems unrealistic due to the noted gap in emissions observed by Probe B

©2014. American Geophysical Union. All Rights Reserved.

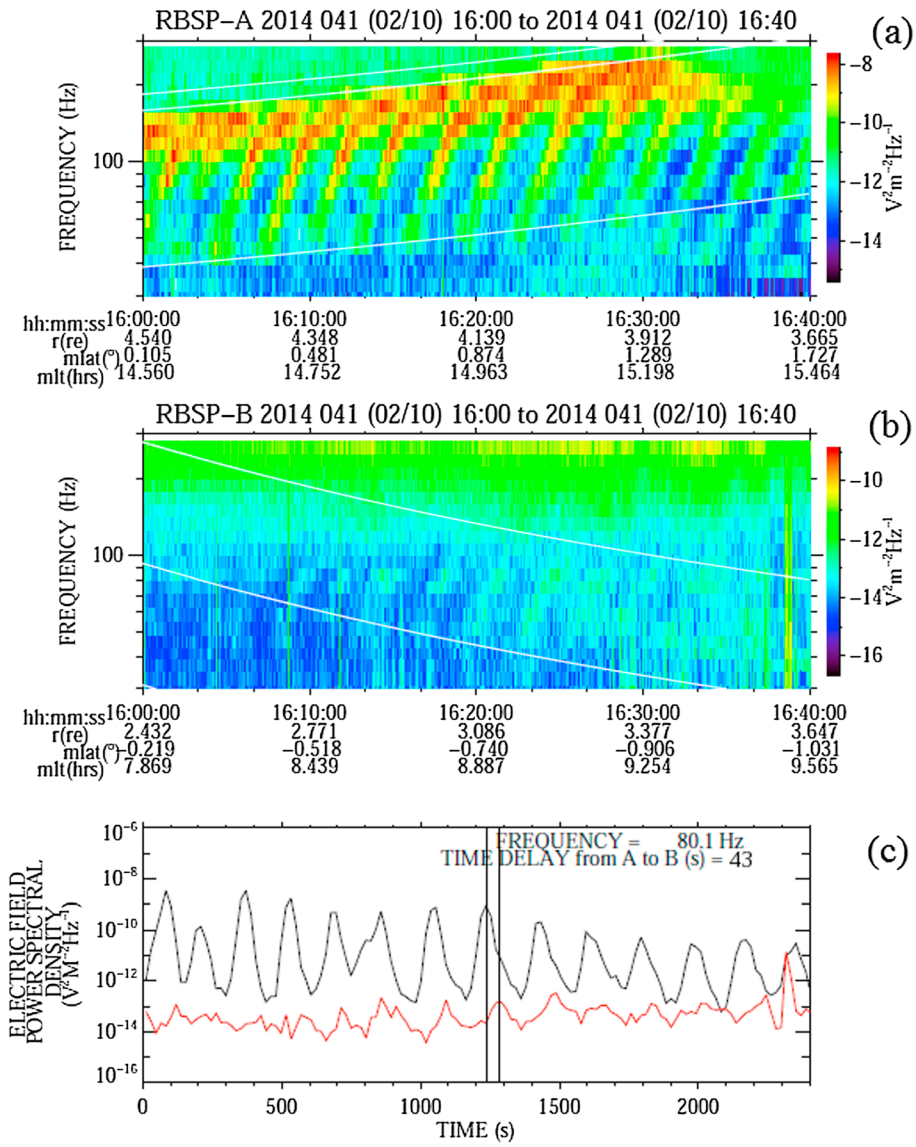

Figure 4. Comparison of concurrent modulated fast magnetosonic mode observed between both spacecraft. Electric field power spectral density from the spin plane antennas for Probes (a) A and (b) B. (c) Estimate of a ~40 s time lag between Probe A (black) and Probe B (red). The white lines in Figure 4a are at 9, 36, and 42 f_{cP}, and in Figure 4b are at 3 and 9 f_{cP}. Probe A is outside and Probe B is inside the plasmapause.

(Figure 3). Moving the source outward in radial distance, say to 6.6 R_E, is a way to substantially increase the rise time, but f_{LHR} at 6.6 is 78 Hz and these emissions are observed up to ~200 Hz.

One possible way to increase the rise time is for the waves to bounce multiple times with the plasmapause wave guide [e.g., *Chen and Thorne*, 2012] or increasing the path length by using an equatorial WNA of say 89°. A wave source localized in magnetic local time but spread out in radial distance from say the plasmapause to geosynchronous might be the another option. Although a ray-tracing study exploring these possibilities might be useful, based on the arguments above we suspect that dispersion can only explain the upper part of each frequency rise where the frequency profile starts to flatten. Due to the noted large discrepancy in the rise time given above, ray tracing probably cannot explain the lower part of the rise in frequency with time. Can ultralow frequency (ULF) waves in the PC 4 to 5 range (45 to 600 s) explain the modulation and the rise time?

For an ULF wave to be the cause of the modulation and lower frequency shift, we reason that two criteria must be satisfied: (1) the wave must create a large periodic variation of V_A to turn on and off the instability

©2014. American Geophysical Union. All Rights Reserved.

and (2) the V_A profile must be nonlinearly steepened creating a sawtooth pattern in time. The latter is required to get the frequency drift. As V_A increases above to the shell velocity the only waves with phase velocities below V_A can be excited, leading to an upward shift in frequency (Figure 1b). We speculate that drifting mirror mode instability detected at 6.6 R_E around noon [see *Kremser et al.*, 1981, Figure 3] might trigger our observations. If the magnetic bubbles formed by this instability generate compressional Alfven waves, the Alfven waves will nonlinearly steepen as they propagate into the plasmapause and if their amplitude becomes large enough, say ~40 nT in 480 nT background field, then the variation in the local V_A should be large enough to turn the fast magnetosonic mode instability on and off in a cyclic manner. Another possibility is the Fast Magnetosonic Resonator [e.g., *Hartinger et al.,* 2014], which can drive quasi-standing fast mode compressional waves between the plasmapause and the magnetopause; these waves occur at frequencies way below the ion cyclotron frequencies. A simulation of this mode along the noontime Sun-Earth line between the plasmapause and the magnetopause is shown in Figures 3a–3d of *Hartinger et al.* [2014],where a strong emission is observed around 5 mHz. However, there are no reported observations of sawtooth ULF 40 nT amplitude waves outside the plasmapause, which surely would have been reported if such strong waves exist. Therefore, we feel that ULF waves being the candidate for the modulation and frequency drift is unlikely.

Another possibility is to draw an analogy with modulated frequency drifting whistler mode emissions whose modulation and frequency drift are attributed to the electron cyclotron maser [e.g., *Trakhtengerts*, 1995; *Pasmanik et al.,* 2004a, 2004b]. To get the modulation of the whistler mode the reasoning is as follows: (1) The source is pitch angle anisotropy in energetic electrons. (2) These electrons become unstable while crossing a field-aligned duct, note that the wave number is along the background field. (3) As the instability turns on, a boundary is formed in pitch angle between isotropic and anisotropic energetic electrons. This boundary moves toward 90° due to pitch angle diffusion causing the unstable wave frequency to increase. (4) When this boundary hits 90°, all the energetic electrons are isotropic and the instability turns off. (5) When enough fresh source electrons flow into the duct, the process restarts leading to a cyclic behavior. If the intensity of the source electrons is sufficiently large, modeling shows that the cyclic pattern will become highly periodic.

For modulated frequency drifting fast magnetosonic mode we reason the following by analogy: (1) The source is freshly injected proton shell distributions. (2) When these distributions drift into a region where the equatorial density contours line up with the magnetic field magnitude contours, they can efficiently tap the free energy source; the wave number is directed along the contours. (3) As the wave intensity increases, strong energy diffusion occurs and the inner edge of the proton shell distribution moves inward in velocity. As the inner edge moves inward the unstable wave frequency increases because V_A is not strongly varying. (4) When the distribution is sufficiently plateaued, the instability turns off. (5) When sufficient source protons flow into this region, the process is restarted leading to cyclic behavior. Further studies are necessary to show whether observations, theory, and modeling can explain these observations.

Acknowledgments
We thank Dave Sibeck for useful discussions and Aaron Roberts (http://hpde.gsfc.nasa.gov/) for providing software that allows one to directly load data sets from the Space Physics Data Facility directly into IDL. These data sets can be obtained from the electronic archive at the Space Physics Data Facility (http://spdf.gsfc.nasa.gov/). This study was supported by NASA prime contract NAS5-01072.

Benoit Lavraud thanks two anonymous reviewers for their assistance in evaluating this paper.

References

Boardsen, S. A., D. L. Gallagher, D. A. Gurnett, W. K. Peterson, and J. L. Green (1992), Funnel-shaped, low-frequency equatorial waves, *J. Geophys. Res.*, *97*, 14,967–14,976, doi:10.1029/92JA00827.

Chen, L., and R. M. Thorne (2012), Perpendicular propagation of magnetosonic waves, *Geophys. Res. Lett.*, *39*, L14102, doi:10.1029/2012GL052485.

Chen, L., R. M. Thorne, V. K. Jordanova, M. F. Thomsen, and R. B. Horne (2011), Magnetosonic wave instability analysis for proton ring distributions observed by the LANL magnetospheric plasma analyzer, *J. Geophys. Res.*, *116*, A03223, doi:10.1029/2010JA016068.

Chen, L., R. M. Thorne, W. Li, J. Bortnik, D. Turner, and V. Angelopoulos (2012), Modulation of plasmaspheric hiss intensity by thermal plasma density structure, *Geophys. Res. Lett.*, *39*, L14103, doi:10.1029/2012GL052308.

Funsten, H. O., et al. (2013), Helium, oxygen, proton, and electron (HOPE) mass spectrometer for the radiation belt storm probes mission, *Space Sci. Rev.*, *179*, 423–484, doi:10.1007/s11214-013-9968-7.

Hartinger, M. D., D. Welling, N. M. Viall, M. B. Moldwin, and A. Ridley (2014), The effect of magnetopause motion on fast mode resonance, *J. Geophys. Res. Space Physics*, doi:10.1002/2014JA020401.

Horne, R. B., G. V. Wheeler, and H. S. C. K. Alleyne (2000), Proton and electron heating by radially propagating fast magnetosonic waves, *J. Geophys. Res.*, *105*, 27,597–27,610, doi:10.1029/2000JA000018.

Kletzing, C. A., et al. (2013), The Electric and Magnetic Field Instrument Suite and Integrated Science (EMFISIS) on RBSP, *Space Sci. Rev.*, *179*, 127–181, doi:10.1007/s11214-013-9993-6.

Korth, A., G. Kremser, S. Perrault, and A. Roux (1984), Interaction of particles with ion-cyclotron waves and magnetosonic waves. Observations from GEOS1 and GEOS2, *Planet. Space Sci.*, *32*(11), 1393–1406.

Kremser, G., A. Korth, J. A. Fejer, B. Wilken, A. V. Gurevich, and E. Amata (1981), Observations of quasi-periodic flux variations of energetic ions and electrons associated with Pc 5 geomagnetic pulsations, *J. Geophys. Res.*, *86*, 3345–3356, doi:10.1029/JA086iA05p03345.

©2014. American Geophysical Union. All Rights Reserved.

Li, W., R. M. Thorne, J. Bortnik, Y. Nishimura, and V. Angelopoulos (2011), Modulation of whistler mode chorus waves: 1. Role of compressional Pc4–5 pulsations, *J. Geophys. Res.*, *116*, A06205, doi:10.1029/2010JA016312.

Loto'aniu, T. M., B. J. Fraser, and C. L. Waters (2009), The modulation of electromagnetic ion cyclotron waves by Pc 5 ULF waves, *Ann. Geophys.*, *27*, 121–130, doi:10.5194/angeo-27-121-2009.

Ma, Q., W. Li1, L. Chen, R. M. Thorne, C. A. Kletzing, W. S. Kurth, G. B. Hospodarsk, G. D. Reeves, M. G. Henderson, and H. E. Spence (2014), The trapping of equatorial magnetosonic waves in the Earth's outer plasmasphere, *Geophys. Res. Lett.*, *41*, 6307–6313, doi:10.1002/2014GL061414.

Meredith, N. P., R. B. Horne, and R. R. Anderson (2008), Survey of magnetosonic waves and proton ring distributions in the Earth's inner magnetosphere, *J. Geophys. Res.*, *113*, A06213, doi:10.1029/2007JA012975.

Pasmanik, D. L., A. G. Demekhov, V. Y. Trakhtengerts, and M. Parrot (2004a), Modeling whistler wave generation regimes in magnetospheric cyclotron maser, *Ann. Geophys.*, *22*, 3561–3570.

Pasmanik, D. L., E. E. Titova, A. G. Demekhov, V. Y. Trakhtengerts, O. Santolik, F. Jiricek, K. Kudela, and M. Parrot (2004b), Quasi-periodic ELF/VLF wave emissions in the Earth's magnetosphere: Comparison of satellite observations and modeling, *Ann. Geophys.*, *22*, 4351–4361.

Perraut, S., A. Roux, P. Robert, R. Gendrin, J.-A. Sauvaud, J.-M. Bosqued, G. Kremser, and A. Korth (1982), A systematic study of ULF waves above F_{H+} from GEOS 1 and 2 measurements and their relationships with proton ring distributions, *J. Geophys. Res.*, *87*, 6219–6236, doi:10.1029/JA087iA08p06219.

Santolík, O., F. Němec, K. Gereová, E. Macúšová, Y. de Conchy, and N. Cornilleau-Wehrlin (2004), Systematic analysis of equatorial noise below the lower hybrid frequency, *Ann. Geophys.*, *22*, 2587–2595, doi:10.5194/angeo-22-2587-2004.

Thomsen, M. F., M. H. Denton, V. K. Jordanova, L. Chen, and R. M. Thorne (2011), Free energy to drive equatorial magnetosonic wave instability at geosynchronous orbit, *J. Geophys. Res.*, *116*, A08220, doi:10.1029/2011JA016644.

Trakhtengerts, V. Y. (1995), Magnetosphere cyclotron maser: Backward wave oscillator generation regime, *J. Geophys. Res.*, *100*, 17,205–17,210, doi:10.1029/95JA00843.

Wygant, J. R., et al. (2013), The electric field and waves instruments on the radiation belt storm probes mission, *Space Sci. Rev.*, *179*(1–4), 183–220, doi:10.1007/s11214-013-0013-7.

©2014. American Geophysical Union. All Rights Reserved.